

The inherent visible light signature of an intense underwater ultraviolet light source due to combined Raman and fluorescence effects

Charles H. Mazel ^{*a}, Jody Kalata-Olson,^b and Chuong Pham ^b

^a Physical Sciences Inc., 20 New England Business Center, Andover, MA 01810

^b Coastal Systems Station, Dahlgren Division, Naval Surface Warfare Center, Panama City, FL 32407

Charles H. Mazel, Jody Kalata-Olson, and Chuong Pham, "The Inherent Visible Light Signature of an Intense Underwater Ultraviolet Light Source Due to Combined Raman and Fluorescence Effects," *Proceedings of SPIE, Information Systems for Divers and Autonomous Underwater Vehicles Operating in Very Shallow Water and Surf Zone Regions II* **4039**, 135-144 (2000).

Copyright © 2000 Society of Photo-Optical Instrumentation Engineers.

This paper was published in *Information Systems for Divers and Autonomous Underwater Vehicles Operating in Very Shallow Water and Surf Zone Regions II (Proceedings of SPIE, 4039)* and is made available as an electronic reprint with permission of SPIE. Single print or electronic copies for personal use only are allowed. Systematic or multiple reproduction, distribution to multiple locations through an electronic listserver or other electronic means, duplication of any material in this paper for a fee or for commercial purposes, or modification of the content of the paper are all prohibited. By choosing to view or print this document, you agree to all the provisions of the copyright law protecting it.

Report Documentation Page				Form Approved OMB No. 0704-0188	
Public reporting burden for the collection of information is estimated to average 1 hour per response, including the time for reviewing instructions, searching existing data sources, gathering and maintaining the data needed, and completing and reviewing the collection of information. Send comments regarding this burden estimate or any other aspect of this collection of information, including suggestions for reducing this burden, to Washington Headquarters Services, Directorate for Information Operations and Reports, 1215 Jefferson Davis Highway, Suite 1204, Arlington VA 22202-4302. Respondents should be aware that notwithstanding any other provision of law, no person shall be subject to a penalty for failing to comply with a collection of information if it does not display a currently valid OMB control number.					
1. REPORT DATE 2000		2. REPORT TYPE		3. DATES COVERED 00-00-2000 to 00-00-2000	
4. TITLE AND SUBTITLE The inherent visible light signature of an intense underwater ultraviolet light source due to combined Raman and fluorescence effects				5a. CONTRACT NUMBER	
				5b. GRANT NUMBER	
				5c. PROGRAM ELEMENT NUMBER	
6. AUTHOR(S)				5d. PROJECT NUMBER	
				5e. TASK NUMBER	
				5f. WORK UNIT NUMBER	
7. PERFORMING ORGANIZATION NAME(S) AND ADDRESS(ES) Physical Sciences Inc,20 New England Business Center,Andover,MA,01810				8. PERFORMING ORGANIZATION REPORT NUMBER	
9. SPONSORING/MONITORING AGENCY NAME(S) AND ADDRESS(ES)				10. SPONSOR/MONITOR'S ACRONYM(S)	
				11. SPONSOR/MONITOR'S REPORT NUMBER(S)	
12. DISTRIBUTION/AVAILABILITY STATEMENT Approved for public release; distribution unlimited					
13. SUPPLEMENTARY NOTES The original document contains color images.					
14. ABSTRACT see report					
15. SUBJECT TERMS					
16. SECURITY CLASSIFICATION OF:			17. LIMITATION OF ABSTRACT	18. NUMBER OF PAGES 11	19a. NAME OF RESPONSIBLE PERSON
a. REPORT unclassified	b. ABSTRACT unclassified	c. THIS PAGE unclassified			

The inherent visible light signature of an intense underwater ultraviolet light source due to combined Raman and fluorescence effects

Charles H. Mazel^{*a}, Jody Kalata-Olson,^b and Chuong Pham^b

^aPhysical Sciences Inc., 20 New England Business Center, Andover , MA 01810

^bCoastal Systems Station, Dahlgren Division, Naval Surface Warfare Center, Panama City, FL 32407

ABSTRACT

We investigated the utility of a portable, intense source of ultraviolet light for diver use in support of Very Shallow Water operations. The working hypothesis was that the light would be of use to divers at short-to-medium ranges (up to several meters) while remaining invisible to surface observers due to the inherent insensitivity of the human eye to ultraviolet light. The light source contained an arc discharge lamp rich in short wavelengths and was fitted with a filter that transmitted only the near ultraviolet portion of the spectrum. In-water tests were made in darkness using Navy divers both in a natural coastal environment and in a test tank. It was found that the light was of limited utility to the divers. In addition, the light was not covert because of a bluish-white glow associated with the ultraviolet beam. Subsequent measurements demonstrated that the visible glow was produced by a combination of fluorescence of dissolved organic matter in the water and Raman scatter from the water itself. The relative importance of the two factors varied with water type. These two effects that transform light from the invisible to the visible impose inherent limitations on the use of ultraviolet light for covert operations.

Keywords: Ultraviolet, Raman, fluorescence, visibility

1. BACKGROUND

We investigated the value of a diver-carried source of ultraviolet light for Navy missions. The hypothesis was that ultraviolet light would provide a useful source of illumination for the diver while minimizing the chance of detection by a surface observer. The reasons for thinking that this might be true were:

- **Use of ultraviolet light would be covert.**
Humans cannot see ultraviolet light. The blue-sensitive cones in the retina would respond weakly to ultraviolet wavelengths if exposed to them, but substances in the lens of the eye filter these out. The light emitted from a properly filtered ultraviolet light source should be invisible to an outside observer.
- **Fluorescence increases contrast.**
Ultraviolet light is effective at stimulating fluorescence (the absorption of electromagnetic radiation at one wavelength and its re-emission at a longer wavelength) in many substances. The resulting light emission is in the visible portion of the spectrum. If a fluorescent object is located in non- or weakly-fluorescing surroundings it will stand out clearly. The ability to detect very small (5 mm diameter and less) biological targets (corals) with fluorescence from distances of several meters has been demonstrated.
- **Ultraviolet light and fluorescence minimize backscatter.**
Backscatter from suspended particles is a major factor limiting detection range when using an active light source. The problem is that the eye or camera is utilizing reflected light, imaging the same wavelengths that are being emitted by the illumination source. Great effort is taken with such systems to separate the light source and the imager to reduce the effect. This problem does not occur in fluorescence because the backscattered ultraviolet light is filtered out, while the visible wavelengths resulting from the fluorescence emission reach the detector unimpeded.

* Correspondence: Email: mazel@psicorp.com; <http://www.psicorp.com>; Telephone: 978 689 0003; Fax 978 689 3232

To explore this hypothesis we constructed a new high intensity underwater ultraviolet light source and conducted controlled field tests with Navy divers and surface observers. This was followed by laboratory investigation of the inelastic optical effects – Raman scatter and fluorescence – that rendered the light source visible.

2. LIGHT SOURCE

A new compact underwater ultraviolet light was built for this project. The light source is a high intensity discharge bulb engineered to be rich in ultraviolet energy. The bulb operates at a steady-state power consumption of 35 W, enabling operation from a diver-carried battery source. The energy between 350 and 400 nm is the longwave ultraviolet (also called UV-A) emission of interest for this project. A Hoya U-360 glass filter mounted in front of the lamp housing restricted the emitted wavelengths to the desired range (Figure 1). The spectral distribution of the light output was measured with an Ocean Optics S2000 spectrometer. The light produced an irradiance of 1 mW/cm² at a distance of 1 m, measured with a UVX Radiometer from Ultra-Violet Products.

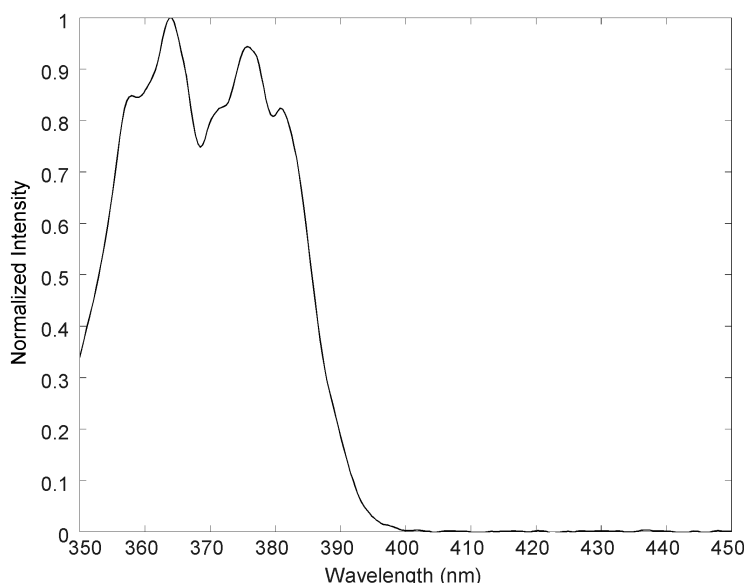


Figure 1. Spectrum of light emitted by the high intensity ultraviolet light source.

3. FIELD TESTS

In-water testing was conducted at two locations at the Navy Coastal Systems Station (CSS), Panama City, Florida: the ammunition pier and the Swimmer Delivery Vehicle (SDV) test tank. At both locations a guide line marked off in uniform distance intervals was laid along the bottom. Fluorescent floats were positioned 1.5 m above the bottom along the guide line. At one end of the line a 1.2 x 1.2 m resolution panel was suspended from the surface and a test object was placed on the bottom. At both locations the water depth was approximately 5 m and the divers were operating 1.5 m above the bottom.

Surface observers were positioned at several locations along the end of the ammunition pier so that they viewed the test area from a range of angles. The pier tests were conducted in full darkness (no moon), with no lights on the pier to interfere with the night vision adaptation of the observers. However, there were shore lights across the bay from the test that caused surface reflections and potentially detracted from viewing the ultraviolet light in the water. The SDV test tank facility was fully darkened and observers were positioned both at the end and along one side of the tank.

At the pier site both the turbidity and the recent input of colored dissolved organic matter (CDOM, also called yellow matter or gelbstoff) from terrestrial runoff were high. The visibility was extremely poor even under daytime ambient light conditions. The SDV test tank was filled with fresh water with a small amount of chlorine added to reduce algae growth. The water appeared fairly clear to the eye, with a slight greenish appearance. At both locations a WET Labs ac-9 absorption-attenuation meter was suspended 2 m from the bottom approximately midway along the guide line and offset to the side by

3 m so that it would not interfere with the divers. The ac-9 measurements from the two sites are summarized in Table 1. The instrument does not measure at ultraviolet wavelengths, but it is known that the attenuation continues to rise as wavelength decreases.

Table 1. Absorption (a) and attenuation (c) coefficients measured at the ammunition pier and at the test tank. Values are time-averaged readings.

Wavelength nm	Pier		Test Tank	
	a, m^{-1}	c, m^{-1}	a, m^{-1}	c, m^{-1}
412	2.35	5.00	0.21	0.41
440	1.80	4.32	0.19	0.36
488	1.17	3.59	0.14	0.32
510	0.98	3.37	0.13	0.30
532	0.84	3.18	0.12	0.31
630	0.55	2.60	0.09	0.27
650	0.51	2.51	0.09	0.27
676	0.54	2.44	0.08	0.26
715	0.38	2.28	0.08	0.26

At the pier site the observers could not see the light while the divers were more than a few feet below the surface. When the divers were very near the surface a pale bluish-white glow was visible to standing observers. The light was less obvious to observers who were seated during the test.

At the SDV test tank the surface observers were able to see the light at all times. As soon as it was turned on it was evident that there was a bluish-white glow associated with the light. This appeared as a faint beam in the water. It was most evident to the observers viewing the divers from above and to the side, so that they were looking perpendicular to the direction of the beam. The beam was visible, but less evident, to the observers looking directly toward the divers along the axis of the beam. The observation of the visible glow associated with the ultraviolet beam was both surprising and disappointing, as it severely compromised the covertness of the light in clear water. The explanation for the glow was not immediately obvious, and we formed two working hypotheses:

1. The glow was from low-level visible light leakage through the ultraviolet-transmitting filter, visible only under the test conditions of full darkness.
2. The glow was the result of inelastic optical interactions in the water.

If the first hypothesis were correct the problem could easily be solved by using a thicker filter or stacking filters to reduce the leakage. If the second hypothesis were correct then there would be no easy way around the problem. Subsequent to the fieldwork at CSS a short test was conducted in a swimming pool. As in the test tank the beam glow was immediately evident. The addition of a second filter reduced the intensity only slightly, indicating the correctness of the second hypothesis.

Samples of water for laboratory analysis were collected from both CSS test sites and from the swimming pool.

4. INELASTIC SCATTER

Inelastic scatter refers to processes that produce a shift in the wavelength (frequency) of incident light. In this instance we consider two of these processes, Raman scatter and fluorescence. Raman scatter results from the interaction of light with the thermal vibrational and rotational states of water molecules.¹ Energy is removed from incident photons by the interaction, resulting in the scatter of photons with longer wavelengths. The interaction is with the water itself, and the magnitude of the resulting frequency shift is predictable. (There are various forms of Raman interaction that can result in other frequency shifts, including shifts to shorter wavelengths, but these are not significant for the case under discussion here.)

In fluorescence an incident photon is absorbed, promoting an electron to an excited state. The electron quickly returns to the ground state, but there is some loss of energy and the resulting emitted photon is at a longer wavelength than the incident

photon. In natural waters the primary sources of fluorescence are CDOM and phytoplankton. CDOM fluoresces roughly in the 400 to 500 nm range,² while phytoplankton fluorescence can occur over a wide range of wavelengths depending on the pigment composition.³ We only consider CDOM fluorescence in this investigation.

The spectral distribution of the Raman signal for any input can be predicted using equations found in reference 1. The relevant factors are the Raman absorption coefficient and the wavelength redistribution function. The Raman absorption coefficient characterizes the wavelength dependence of the fraction of incident light that will be Raman-shifted.

$$a^R(\lambda') = a_0^R \left(\frac{\lambda_0'}{\lambda'} \right)^4, \quad (1)$$

where $a^R(\lambda')$ is the Raman absorption coefficient at wavelength λ' and $a_0^R = 5.8 \times 10^{-4} \text{ m}^{-1}$ is the Raman absorption coefficient at wavelength $\lambda_0' = 400 \text{ nm}$.¹

The wavelength redistribution function is a probability density function that characterizes the Raman emission at any wavelength $\lambda > \lambda'$ for any given input wavelength λ' (λ and λ' in nm).

$$f^R(\lambda' \rightarrow \lambda) \equiv \frac{10^7}{\lambda^2} f^R \left[10^7 \left(\frac{1}{\lambda'} - \frac{1}{\lambda} \right) \right]. \quad (2)$$

(The function $f^R(\kappa')$ embodied in the right-hand side of this equation is equation 5.92 in reference 1 and is omitted here.)

The spatial distribution of the emission will be governed by the Raman scattering phase function, which is symmetrical about its minimum at 90 deg.¹

The absorption coefficient for CDOM can be estimated from

$$a_y(\lambda') = a_y(\lambda_o) e^{[-0.014(\lambda' - \lambda_o)]} \quad (3)$$

where the reference wavelength λ_o is commonly selected to be 440 nm.¹ A reasonable approximation for the fluorescence efficiency (quanta fluoresced divided by quanta absorbed) is 0.01.² The spectral distribution of the emitted photons will vary depending on the source of the CDOM and the balance between humic and fulvic acid.² It will be determined here by measurement. The phase function for fluorescence emission is taken to be isotropic.¹

5. LABORATORY MEASUREMENTS

Measurements of the emission from the field samples and from distilled water were made using a FluoroMax-2 Spectrofluorometer (SPEX Industries). Instrument settings were: excitation wavelength 370 nm, scan range 380 to 500 nm, integration time 0.3 sec, 5 nm bandpass slits, dark offset correction, ratio correction mode. The measurements were corrected for detector spectral sensitivity. The results are shown in Figure 2. The signal from distilled water is due only to Raman emission. For the field water samples the emission is a combination of water Raman and fluorescence from CDOM. The results are replotted in Figure 3 with the Raman signal subtracted.

The measurements indicate that water Raman is a significant component of the light emitted by the water. For the pier water sample there is a strong fluorescence from the CDOM that we expect to be associated with a location that has regular input of terrestrial runoff. In this case the Raman emission appears as a bump in the signal. The test tank was substantially cleaner than the pier water, and the sample exhibits lower fluorescence from CDOM, with a consequent higher relative contribution from Raman. In the case of the swimming pool water the Raman scatter appears to be the dominant effect.

The spectrofluorometer measurements were made at only one excitation wavelength. The ultraviolet light source emits in the range of 350 to 400 nm. Each wavelength in that band would excite both Raman and fluorescence emission, with the relative amounts varying as a function of input wavelength.

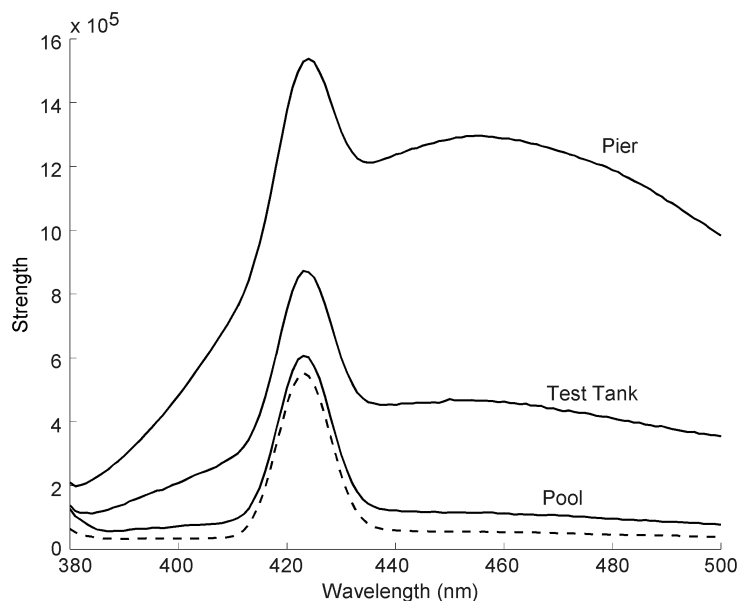


Figure 2. Spectrofluorometer measurements of distilled water (dashed line) and water samples from the ammunition pier, SDV test tank, and swimming pool.

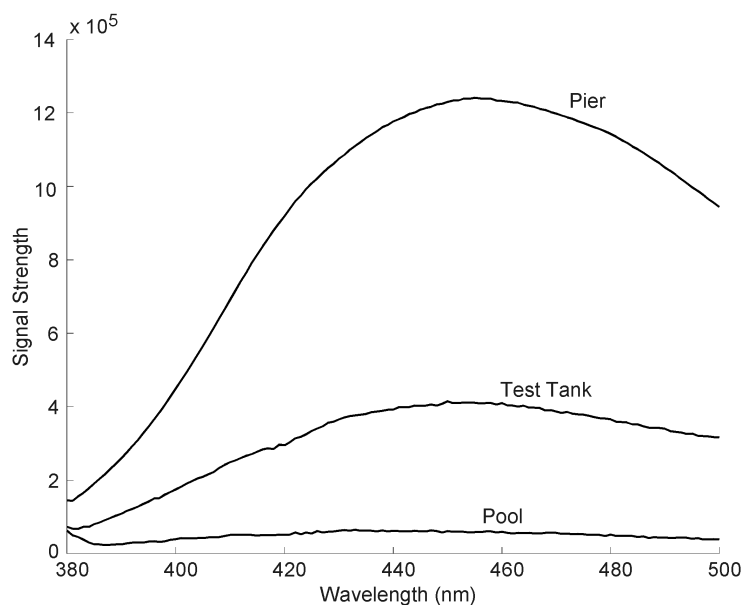


Figure 3. Spectrofluorometer measurements of water samples from the ammunition pier, SDV test tank, and swimming pool. The distilled water Raman signal has been subtracted from the data for the other samples.

In the laboratory we directed the beam of the ultraviolet light into a small aquarium tank filled with distilled water. A faint purple glow was evident to the eye. We directed the measurement fiber of the FluoroMax spectrofluorometer normal to the light path through the water to measure the scattered light. The data (Figure 4) show that some of the light is incident light that has undergone elastic scatter, and some is light that has been inelastically scattered to longer wavelengths. Figure 5 shows the comparison of the inelastically shifted portion of Figure 4 to the Raman spectral distribution calculated by applying Eqs. (1) and (2) to the spectrum of the incident light (Figure 1). The agreement is very good, confirming that we are seeing Raman as a portion of the scattered light.

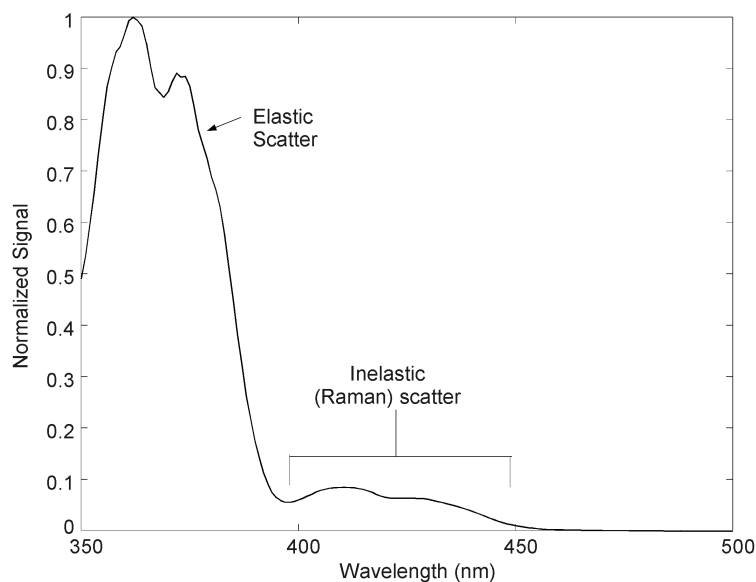


Figure 4. Scattered light in distilled water, measured normal to the beam axis.

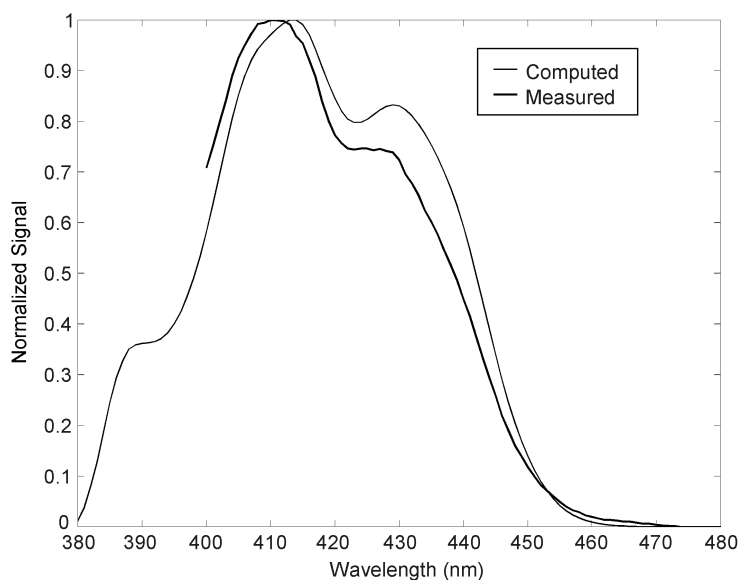


Figure 5. Comparison of inelastic scatter portion of Figure 4 with the Raman spectral distribution computed from the spectral distribution in Figure 1.

According to reference 1 ‘roughly one in ten photons scattered by water molecules is Raman-scattered to another wavelength.’ Note the emphasis that this statement applies only to scattering from water molecules, as light scattered from particulates in the water would not be Raman-shifted in the same manner. The data plotted in Figure 4 were collected from distilled water, and the magnitude of the elastic-scattered peak in the ultraviolet is on the order of ten times greater than the inelastic-scattered peak, as expected. For field water samples we would also have to take into account particulate scatterers, which would tend to increase the relative amplitude of the elastically scattered component.

The experiment was repeated using tap water instead of distilled water in the aquarium tank. The beam appeared a weak purple with distilled water and was noticeably ‘whiter’ with tap water. Even tap water contains trace amounts of dissolved

organic matter that contribute a fluorescence component to the signal. Our conclusion is that the bluish-white glow associated with the light even in clear water is the result of both Raman and fluorescence.

6. QUANTITATIVE ESTIMATE OF VISIBLE SIGNATURE

From the prior section we know that the energy in the ultraviolet beam is partially converted to visible wavelengths by the combined inelastic effects of Raman scatter and fluorescence. We can make a rough estimate of the magnitude of the visible light signature by making several simplifying assumptions. We will assume that: the beam is directed into the water horizontally and is not striking any discrete surfaces that would produce significant reflections; that the beam is collimated, so that no direct emission from the light source will reach the surface; that the only attenuating effects are absorption by water and CDOM; and that all of the light output is at 375 nm (the approximate middle of the measured light spectrum (Figure 1)).

If the beam produces an irradiance I ($\text{W}\cdot\text{m}^{-2}$) and has a cross-sectional area A (m^2) then the radiated power will $P_0 = A * I$ (W). The power reaching any distance x from the light source will be $P_x = P_0 e^{-ax}$, where a will be the sum of the water and CDOM absorption coefficients. In a 1 cm cross section along the beam axis the power removed from the beam, P_r , by absorption will be

$$P_r = P_x (1 - e^{-0.01a}) . \quad (4)$$

The a in this equation would properly be the sum of the absorption coefficients, at 375 nm, for water and CDOM, but the error is small if we deal with the contributing absorption effects individually, substituting the appropriate coefficients into this equation in turn to compute the power removed by any particular mechanism. The pure water absorption, a_w , is approximately 0.026 m^{-1} .¹ The CDOM absorption coefficient can be estimated by substituting $\lambda' = 375$ in Eq. (3). The value of $a_y(440)$ will vary with the amount of CDOM present.⁴ Furthermore, for small values of a , as will be the case here, $(1 - e^{-0.01a}) \approx 0.01a$.

The absorption to Raman is a component of the pure water absorption. Substituting $\lambda' = 375$ nm in (1) yields $a^R = 7.5 \times 10^{-4} \text{ m}^{-1}$, and substituting this in (4), with the simplification noted above, yields $P_R = 7.5 \times 10^{-6} P_x$ for the power removed to Raman scatter. We can express this in photons per second by dividing the power by the energy per photon ($E = \hbar c / \lambda'$, where \hbar is Planck's constant and c is the speed of light). The same photon flux will appear as Raman-shifted photons in the visible spectrum.

Similarly, the power removed in the 1 cm cross-section by yellow matter absorption is $0.01a_y P_x$, and this can be converted to a photon flux by dividing by the energy per photon. The number of photons emitted as fluorescence will be determined by the quantum efficiency, which we have noted will be approximated by 0.01.

Once the inelastically scattered photons leave the beam they will travel through the water column to the observer. For an observer at a distance we will assume that the section through the beam acts as a point source. This behavior has been treated in detail,⁵ with the conclusion that for an observer roughly above the source the irradiance distribution produced at the surface is governed mostly by absorption and geometry, with scattering playing a negligible role. There will also be refraction effects as the light passes through the air-water interface, but those will be neglected here. We will assume spherical spreading over the full source-to-observer range and absorption in the water column. We will use 420 nm as the proxy wavelength to select the absorption coefficient for the Raman scatter, and 460 nm as the proxy for the CDOM fluorescence emission. If we assume isotropic phase functions for both Raman and fluorescence the emitted light will spread to a sphere with surface area $4\pi R^2$ at beam-to-observer range R . If the detector is a human eye, then the aperture will be the pupil area, $\pi p^2/4$, where p is the pupil diameter (approximately 8 mm for a dark-adapted human eye). The fraction of the emitted light that will be intercepted is then $p^2/16R^2$.

With these simplifying assumptions we can estimate the photon flux leaving the 1 cm thick slab and reaching the observer's eye. The only factor we are varying is the absorption by CDOM, so the results will be plotted as a function of that variable, represented by the absorption at 440 nm.

Figure 6 is a plot of the inelastically scattered photon flux produced in a 1 cm slab of the outgoing light beam, at a distance of 50 cm from the source. With no CDOM ($a_y(440) = 0$) only Raman scatter is producing visible photons. The Raman-shifted photon flux will be a constant fraction of the incident flux, and will therefore decrease as absorption by CDOM decreases that incident flux. Emission by fluorescence increases rapidly as CDOM increases, but then decreases as the incident flux is reduced by the same absorption processes. The range of $a_y(440)$ can be considered to represent a transition from clear oceanic waters to coastal waters containing dissolved humic and fulvic substances. Note that the results are computed at a distance of 50 cm from the source. For any given value of $a_y(440)$ the inelastic scatter would be stronger at positions closer to the source, and decrease with distance along the beam.

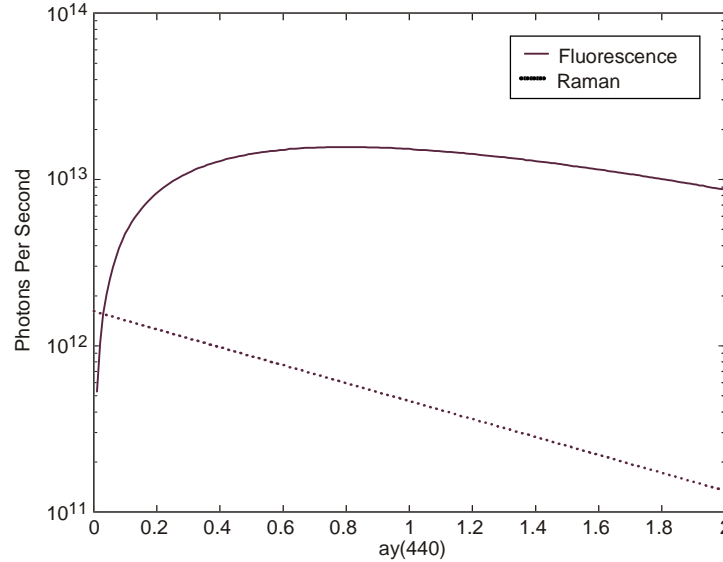


Figure 6. Flux of Raman-shifted and fluoresced photons leaving a 1 cm slab of the ultraviolet light beam at a distance of 50 cm from the source, plotted against CDOM absorption ($a_y(440)$).

Figure 7 displays the photon flux passing through the aperture of the observer's eye as a function of CDOM absorption and depth of the light source. The observer is considered to be 2 m above the water surface, producing additional signal weakening by spreading but not by absorption. As expected, the signal becomes weaker with increasing depth to the light source and increasing water absorption.

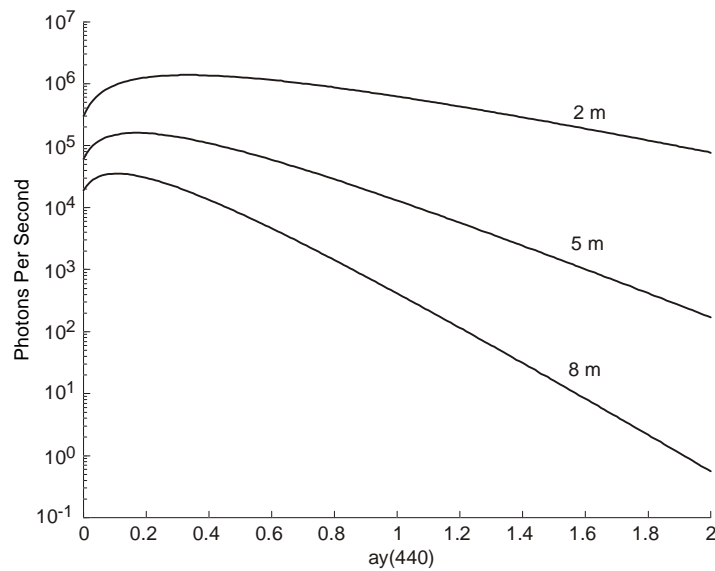


Figure 7. Total flux of visible-wavelength photons reaching an area the size of a dark-adapted pupil for several operating depths of the ultraviolet light source, plotted against CDOM absorption ($a_y(440)$).

Finally, it is worth considering the relation between the Raman-shifted and fluoresced photons and the sensitivity of the human eye. Figure 8 shows normalized wavelength distributions of the photons produced by Raman and by fluorescence and the scotopic luminosity function $V(\lambda)$,⁶ the relative spectral sensitivity of the rod cells. It is the rods that function at low light levels in the dark-adapted eye. The CDOM fluorescence data were measured from a natural water sample with 370 nm excitation. It is evident that the eye is more sensitive to the wavelengths produced by fluorescence than those resulting from the Raman shift of the original ultraviolet. Since humans can perceive as few as seven photons under the proper circumstances, it is also clear that under most combinations of light source depth and water quality there will be more than enough visible-shifted photons to render the ultraviolet light source visible to surface observers.

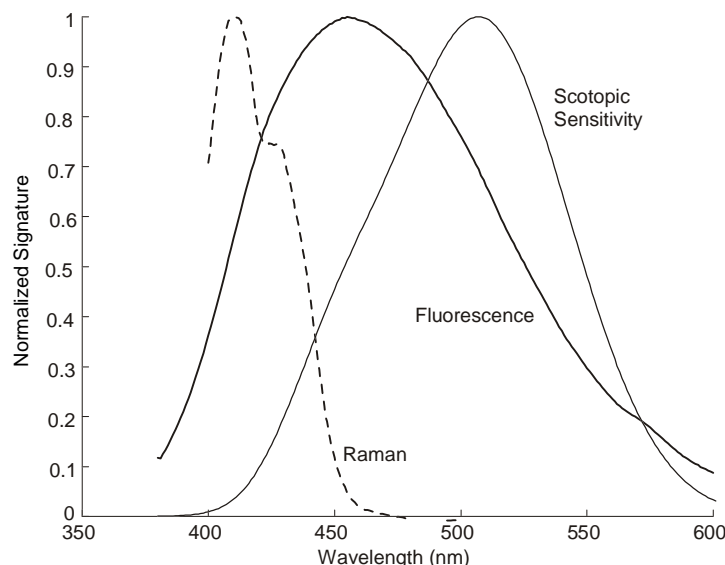


Figure 8. Scotopic luminosity function (thin line) and the spectral distributions of photons arising from fluorescence (thick line) and Raman.

7. DISCUSSION

The experimental and mathematical results presented here demonstrate that the processes of Raman scatter and fluorescence will create a visible signature from an otherwise invisible ultraviolet beam. Under most conditions there will be enough water-leaving photons for the beam to be seen by a surface observer.

In the treatment here we have neglected the effects of attenuating processes other than absorption by water and CDOM. The effect of adding other absorbers and scatterers would be to reduce the photon flux in the original ultraviolet light beam and increase the attenuation of inelastically-shifted photons as they propagate to the surface. Phytoplankton, for example, would have some effect on the ultraviolet attenuation due to the weak absorption in that wavelength range,¹ but would have a stronger impact on the photons in the mid-400 nm range. Scattering processes would tend to weaken the beam further. There are also phytoplankton sources of fluorescence in the 400 to 500 nm range,^{3,7} but their distribution is not well known and their fluorescence properties not well characterized.

Several authors^{3,8,9} have considered the contributions of Raman and in fluorescence in regard to measurements of irradiance reflectance under solar illumination. They reach a similar conclusion that the relative contributions of the two factors will vary with wavelength, water type and the concentration of CDOM and other sources of fluorescence.

8. ACKNOWLEDGMENTS

This work was supported by the Office of Naval Research under Contract N0014-9-M-0083.

9. REFERENCES

1. C. D. Mobley, *Light and Water*, Academic Press, San Diego, 1994.
2. S. K. Hawes, K. L. Carder, and G. R. Harvey, "Quantum fluorescence efficiencies of marine humic and fulvic acids," *Proc. of First Thematic Conference on Remote Sensing for Marine and Coastal Waters*, SPIE Vol. 1930, pp. 533-545, 1992.
3. C. S. Yentsch, and D. A. Phinney, "Autofluorescence and Raman scattering in the marine underwater environment," *Ocean Optics X*, SPIE Vol. 1302 pp. 328-334, 1990.
4. J. T. O. Kirk, "Light and Photosynthesis in Aquatic Ecosystems," Cambridge University Press, 401 pp., 1983.
5. H. R. Gordon, "Bio-optical model describing the distribution of irradiance at the sea surface resulting from a point source embedded in the ocean," *Appl. Opt.* **26**, pp. 4133-4148, 1987.
6. G. Wyszecki and W. S. Stiles, *Color Science: Concepts and Methods, Quantitative Data and Formulae* (2nd ed.), Wiley, New York, 1982.
7. L. P. Shapiro, E. M. Haugen and E. J. Carpenter, "Occurrence and abundance of green-fluorescing dinoflagellates in surface waters of the northwest Atlantic and northeast Pacific oceans," *J. Phycol.* **25**, pp. 189-191, 1989.
8. R. H. Stavn, "Raman scattering effects at the shorter visible wavelengths in clear ocean waters," *Ocean Optics X*, SPIE Vol. 1302 pp. 94-100, 1990.
9. T. G. Peacock, K. L. Carder, C. O. Davis and R. G. Steward, "Effects of fluorescence and water Raman scattering on models of remote sensing reflectance," *Ocean Optics X*, SPIE Vol. 1302 pp. 303-319, 1990.